

Annealing Temperature Effect on Structural and Luminescence Spectroscopy of $Y_2SiO_5:Ce^{3+}$ Nanomaterial Synthesized by Sol–Gel Method

M.S.E. Hamroun^{1,2,*}, A. Guenanou¹, L. Guerbous³, R. Chebout¹ and K. Bachari¹

¹Centre de Recherche Scientifique et Technique en Analyses Physico-Chimiques, BP 384, Zone Industrielle, Bou-Ismaïl CP 42004, Tipaza, Algeria

²Macromolecular Research Laboratory, Faculty of Sciences, Abou Bekr Belkaid University, Chetouane, P.O. Box 119, 13000 Tlemcen, Algeria

³Laser Department/Nuclear Research Centre of Algiers (CRNA), 02 Boulevard Frantz Fanon, P.O. Box 399, 16000 Algiers, Algeria

Abstract: Ce^{3+} -doped Y_2SiO_5 nanophosphors were successfully produced by Sol-Gel process. To study the influence of the temperature on the structure and the luminescence of $Y_2SiO_5:Ce^{3+}$, we annealed the xerogels at the temperatures 800, 900, 950, 1000, 1050 and 1250 °C. The X-ray diffraction technique (XRD), field emission scanning electron microscopy (FEG-SEM), Fourier transform infrared spectroscopy (FTIR) and steady photoluminescence were used to characterize the samples. The crystallite size keeps the same value in the temperature range 950-1050 °C. The room temperature steady photoluminescence emission and excitation of Ce^{3+} in $X_1-Y_2SiO_5:Ce^{3+}$ nanomaterial with increasing temperature were measured and investigated. At the crystallization temperature of 1250 °C, we have a new structure $X_2-Y_2SiO_5:Ce^{3+}$ with grain sizes larger than the $X_1-Y_2SiO_5:Ce^{3+}$ and also intense violet-blue emission.

Keywords: $X_1-Y_2SiO_5$, $X_2-Y_2SiO_5$, nanophosphors, sol–gel, photoluminescence, cerium.

1. INTRODUCTION

The cerium Ce^{3+} doped rare earth (R) oxyorthosilicates (R_2SiO_5) have been subject to intensive studies as cathodoluminescence and storage phosphors as well as scintillators [1]. The development in the field of inorganic materials doped with luminescent rare earth ions has steadily increased from one year to another. Recently, with great progress of nanomaterials fabrication, one-dimensional optical materials, such as nanowires and nanotubes, have attracted great interests as the fundamental blocks for building various optoelectronic nano-devices, nano-lasers, sensors, polarized luminescence, etc [2]. The yttrium silicate (Y_2SiO_5) possesses desirable thermodynamic, dielectric, and structural properties, which makes it attractive as a candidate for high dielectric constant insulators [3]. It is known that Ce^{3+} presents only one optically active electron and exhibits the simplest energy-level structure among all trivalent rare-earth ions. Therefore, it is particularly suitable for use as a model to investigate the effect of the crystalline environment on the luminescence properties. Among these materials, cerium Ce^{3+} -doped

rare-earth (R) oxyorthosilicates (R_2SiO_5) host materials have been the subject of intensive studies for several applications such as cathode luminescence and storage phosphors as well as scintillators [4].

Sol–gel chemistry offers very unique tools for nanoscale mastering of the materials preparation [5].

In the previous work [4] we studied the influence of the monomer and polymers on structural, morphological and photoluminescence spectra of Ce^{3+} ions doped $X_1-Y_2SiO_5$.

In this work, we focus to study the effect of the thermal annealing temperature on the structure and the photoluminescence of $Y_2SiO_5:Ce^{3+}$ assisted by organic complex polymer of Polyethylene glycol.

2. EXPERIMENTAL

2.1. Samples Preparation

The $Y_2SiO_5: 1 \text{ at } \% Ce^{3+}$ ($Y_{1.98}Ce_{0.02}SiO_5$) samples were prepared by sol–gel method. The yttrium oxide (Y_2O_3 , 99,999 %, Fluka Chemika) and cerium (III) nitrate hexahydrate ($Ce(NO_3)_3 \cdot 6H_2O$, 0, 99 %, Biochem Chemopharma) were dissolved in 100 ml of deionized water and 3 ml of nitric acid (HNO_3). After the mixed solution was stirred at room temperature, we add

*Address correspondence to this author at the Macromolecular Research Laboratory, Faculty of Sciences, Abou Bekr Belkaid University, Chetouane, P.O. Box 119, 13000 Tlemcen, Algeria; E-mail: ms.hamroun@gmail.com, msalah.hamroun@crapc.dz

tetraethyl orthosilicate (TEOS, $\text{SiC}_8\text{H}_{20}\text{O}_4$, 99.0 %, Sigma-Aldrich) precursor of silicate. In the resulting solution, we added an organic complex Ethylene glycol (Fluka) in 1:1 mass ratio to the expected mass of the final product and stirred for 1 h at room temperature. The pH was adjusted to 7 by slowly adding ammonia solution and stirring until gel was obtained. Drying is performed at 120 °C for 2 days. Finally, the powders were introduced in a furnace and heated in air at different temperature 800, 900, 950, 1000, 1050 and 1250 °C during 4 h for each sample.

2.2. Characterization

The phase identification and the related properties of the nanopowders were investigated by X-ray diffraction (XRD) technique a PAN analytical X'Pert (Philips) PRO using $\text{CuK}\alpha$ radiation ($\lambda = 1.540 \text{ \AA}$) operated at 45 kV and 40 mA. A symmetric (θ - θ) scans were performed from 10° to 80° 2θ with a step width of 0.02°. The morphology of the powders has been studied by scanning electron microscopy (SEM) (SEM, Philips XL-30). The infrared spectra were recorded in the range of 400-4000 cm^{-1} with a Nicolet-IR 380 Fourier transform infrared (FTIR) spectrometer. The photoluminescence spectra were carried out using Perkin-Elmer (LS-50B) luminescence spectrometer using Xe lamp with excitation wavelength at room temperature as described in ref [6].

3. RESULTS AND DISCUSSION

3.1. XRD Study

Figure 1 show the X-ray diffraction patterns of $\text{Y}_{1.98}\text{Ce}_{0.02}\text{SiO}_5$ (Y_2SiO_5 : 1 at% Ce^{3+}) synthesized by the sol-gel method and annealed at different temperatures namely, 800, 900, 950, 1000 and 1050 °C. From these results, it can be seen that the sample annealed at 800 °C for 4 hours, show a wide band of low intensity centered around 30° (2θ), which translates the amorphous structure. For a heat treatment at 900 °C, less intense peaks are observed. In this case, we can say that we have the beginning of the formation of the crystal structure $\text{X}_1\text{-Y}_2\text{SiO}_5$. On the other hand, Cannas *et al.* [7] studied the properties of $\text{X}_1\text{-Y}_2\text{SiO}_5$ powders doped with Eu^{3+} (Europium) ions produced by the sol-gel method; They varied the annealing temperature from 900 to 1300 °C and found that 1000 °C corresponded to the starting crystallization temperature. From the 950 °C temperature, we have narrower and better defined peaks that define the $\text{X}_1\text{-Y}_2\text{SiO}_5$ phase with space group monoclinic $\text{P}2_1/\text{c}$

(JCPDS N° 00-52-1810 Card); we find that the diffraction peaks intensities increases with the thermal annealing temperature, which indicate better crystallinity. The heat treatment of 4 hours at 1050 °C retains the same structure of the $\text{X}_1\text{-Y}_2\text{SiO}_5$ phase, which proves that a stable phase is reached up to this temperature. And what is important in our results is that there is no trace of the parasites phases of Y_2O_3 or $\text{Y}_2\text{Si}_2\text{O}_7$ in the structure, which shows that we are arrived to elaborate a pure phase of Y_2SiO_5 .

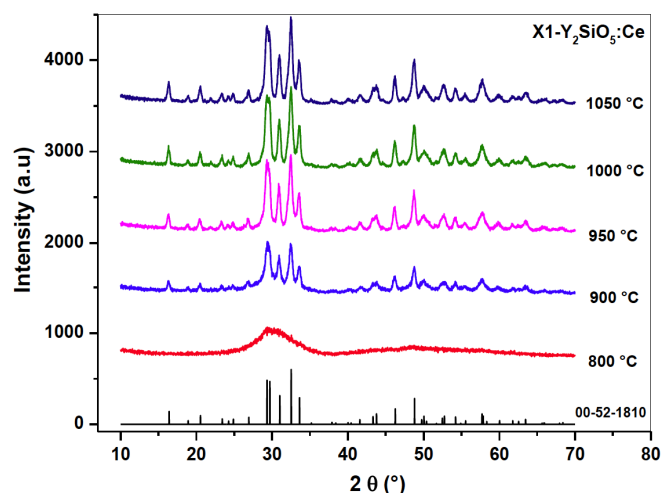


Figure 1: DRX spectra of $\text{X}_1\text{-Y}_2\text{SiO}_5$: Ce^{3+} with different annealing temperature 800, 900, 950, 1000, 1050 °C for 4 h.

Figure 2 shows the X-ray diffractogram on the Ce^{3+} - doped Y_2SiO_5 sample and annealed at 1250 °C for 4h. The diffractogram is composed of fine lines which have been indexed in accordance with the monoclinic phase of the $\text{C}2/\text{c}$ space group (JCPDS 00-036-1476) corresponding to the $\text{X}_2\text{-Y}_2\text{SiO}_5$ phase. In addition, two peaks corresponding to the parasite phase $\text{Y}_2\text{Si}_2\text{O}_7$ are observed on the X-ray diffraction spectrum.

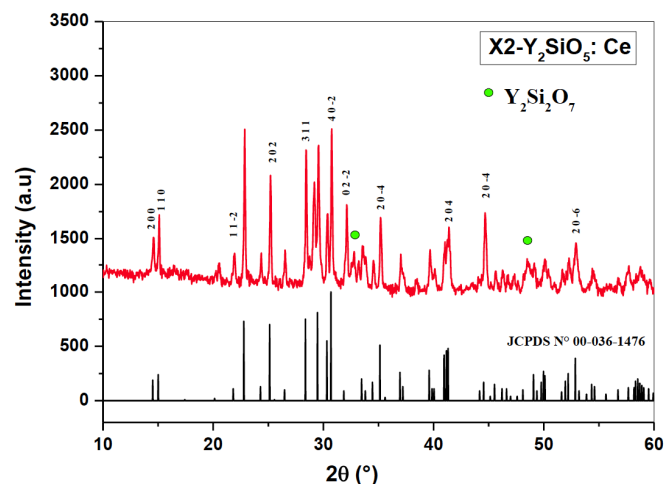


Figure 2: DRX spectra of $\text{X}_2\text{-Y}_2\text{SiO}_5$: Ce^{3+} annealed at 1250 °C for 4 h.

We have determined the crystallite size of all annealed samples using X-ray diffractograms results and both Scherrer, Williamson-Hall approaches. The D_{Sch} is calculated from the diffraction peak corresponding to the (2 0 -2) plane of the $X_1-Y_2SiO_5$ and (2 0 2) for $X_2-Y_2SiO_5$. Also, for the calculation of D_{W-H} we used the first five most intense peaks of the X-ray diffractograms. The crystal lattice strain generated by the annealing temperature is determined from the Williamson–Hall relationship equation (1) [8]:

$$\beta \times \frac{\cos \theta}{\lambda} = \frac{1}{D} + \eta \sin \theta / \lambda \quad (1)$$

D_{W-H} is the effective crystallite size on Williamson–Hall model, η is the effective strain, k is shape factor (0.9), λ is the wavelength of the X-rays (0.154056 nm), θ is the diffraction angle and β is the full half width maximum (FWHM) of the pure diffraction profile in radians.

Table 1 groups together the values of the average crystallite size and the calculated crystallographic parameters. From the results obtained shown in Table 1, the experimental crystallographic parameters are confirmed by JCPDS cards 00-52-1810 and 00-036-1476 for each structure. We note that the size of the crystallites calculated by the Williamson-hall model ($D_{w-s} = 41$ nm) is greater than that calculated by the Sherrer model ($D_{sh} = 28$ nm). This is explained by the fact that there is a high stress value acting on the crystal lattice of the structure Y_2SiO_5 ($\eta = 0.013$).

From the results shown in Table 1, it is noted that although the annealing temperature increases from 950 to 1050 °C, the crystallite size and strain of the samples is nearly constant. One can explain that when the temperature increases, new isolated crystallites are

generated from amorphous material instead of the coalition phenomenon between the former nanocrystallites.

The $X_2-Y_2SiO_5:Ce^{3+}$ sample (annealed at 1250 °C) has larger crystallite sizes (~ 88 nm) compared with the $X_1-Y_2SiO_5:Ce^{3+}$ samples (~ 41 nm). This is because of the temperature of the heat treatment of $X_2-Y_2SiO_5:Ce^{3+}$ and which gives it a significant growth compared to $X_1-Y_2SiO_5:Ce^{3+}$. The cell volume of $X_2-Y_2SiO_5:Ce^{3+}$ (853 Å³) is also larger than that in the case of phase $X_1-Y_2SiO_5:Ce^{3+}$ (399 Å³) which shows difference between these two phases.

3.2. Temperature Effect on Infrared Spectroscopy (FTIR) Spectra

It is known that organic residues give rise to serious effects on luminescence efficiency and sometimes still remain in the nanopowders inevitably. It is well known that FTIR technique is an effective method to reveal the composition of products. The infrared spectra of $Y_2SiO_5:Ce^{3+}$ powder samples annealed at 900 and 1050 °C for 4 h are given in Figure 3. All infrared spectra possess the same inorganic silicates characteristic as strong band centered around 1100 cm⁻¹ that appear as multiple bands of SiO₄ at 1020, 953, 883 and 858 cm⁻¹, suggesting the formation of well-crystallized silicate are observed [4]. Furthermore, the bending bands of SiO₄ at 562 and 435 cm⁻¹ are observed [5]. The absorption peak at 490 cm⁻¹ is due to bonding vibrations of Y-O bonds [4]. There was no difference between the bands observed in the 500-3000 cm⁻¹ range for the two samples annealed at 900 and 1050 °C. We observe also a wide band at 3402 cm⁻¹ corresponds to the O-H bond in the annealed sample at 900 °C and which decreases when the temperature is raised to 1050 °C. As is known, the

Table 1: Grain Size and Crystallographic Parameters of Samples $Y_2SiO_5:Ce^{3+}$ Annealing at Different Temperatures

	a(Å)	b(Å)	c(Å)	V(Å ³)	β (°)	D_{sh} (nm)	D_{w-h} (nm)	ξ
$X_1-Y_2SiO_5:Ce^{3+}$ 900 °C	9	6.93	6.64	397.07	106.67	21	28	0,0052
$X_1-Y_2SiO_5:Ce^{3+}$ 950 °C	9.01	6.935	6.665	398.87	106.77	28	41	0.012
$X_1-Y_2SiO_5:Ce^{3+}$ 1000 °C	9.01	6.92	6.66	398.52	106.71	30	41	0.011
$X_1-Y_2SiO_5:Ce^{3+}$ 1050 °C	9	6.96	6.65	399.42	106.53	28	41	0.013
$X_2-Y_2SiO_5:Ce^{3+}$ 1250 °C	12.5	6.73	10.41	853.91	102.65	84	88	8E-4

presence of the O-H bond in the structure reflects the weakening of the emission of the material.

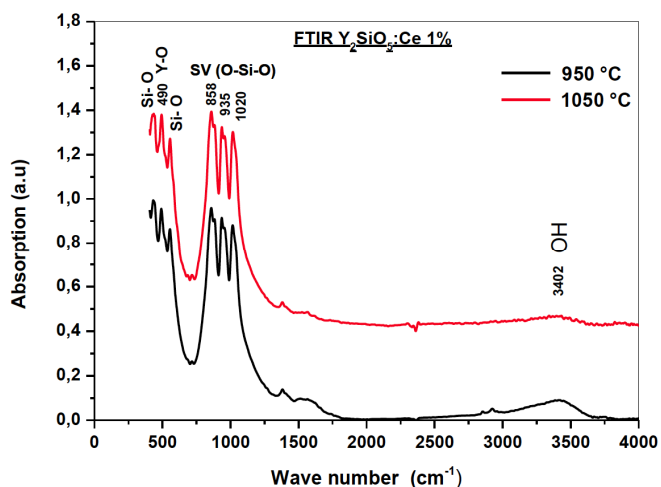


Figure 3: Infrared spectra of samples X_1 -Y $_2$ SiO $_5$:Ce $^{3+}$ annealed at 950 and 1050 °C.

3.3. Morphology

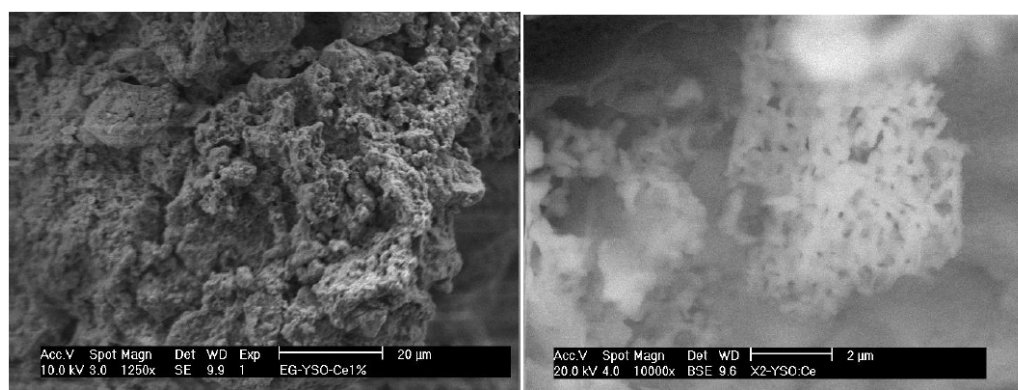
Figure 4 shows the morphology of Y $_2$ SiO $_5$:Ce $^{3+}$ powders heated at 1050 and 1250 °C for 4 h and reveals agglomerate particles and broad asymmetrical particle size distribution, with irregular morphology free of pores.

3.4. Photoluminescence Spectroscopy

Figure 5 shows the emission spectra measured at a wavelength of excitation 360 nm of the phosphor powders Y $_2$ SiO $_5$:Ce $^{3+}$ prepared by the sol-gel process and annealed at different temperatures 800, 900, 950, 1000, 1050 and 1250 °C for 4 hours. We clearly see that the sample annealed at 800 °C shows no emission, which is evident and can be explained by the fact that the structure of the sample remained

amorphous at this annealing temperature and what is also confirmed by the XRD technique. From 900 °C, the crystallization of the X $_1$ -Y $_2$ SiO $_5$:Ce $^{3+}$ matrix begins to take place. At this stage, the broadband corresponding to the transition 5d \rightarrow 4f characteristic of the emission of the Ce $^{3+}$ ion in the X $_1$ -Y $_2$ SiO $_5$ phase begins to be refined, indicating that a large percentage of the material has been crystallized at this temperature. We have observed that the emission intensity of our samples increases progressively with the temperature of the heat treatment, and which is of a maximum intensity at the temperature 1050 °C. In fact, one can thought that this phenomenon can be explained by the improvement of the quality crystallinity, which leads to better a substitution of the Ce $^{3+}$ ions in the Y $^{3+}$ sites in the crystal lattice with the increase in temperature. In addition, at low annealing temperatures, a killer centers namely NO $_3$ and OH molecules presents in samples can losing Ce $^{3+}$ emission in the X $_1$ -Y $_2$ SiO $_5$ host material. In the case of the sample annealed at 1250 °C, we note that the emission spectrum consists of a broad and asymmetric emission band centered at 420 nm and of greater luminescent intensity compared to the other samples.

There is also a high energy shift (redshift) for the two emission spectra (1050 °C and 1250 °C) in Figures 6 and 7. This is due to the presence of Ce $^{3+}$ ions in different crystallographic sites of Y $_2$ SiO $_5$ and that the center of gravity of the excited levels 5d and the emission bands of Ce $^{3+}$ are at lower energies in X $_1$ -Y $_2$ SiO $_5$ than X $_2$ -Y $_2$ SiO $_5$ (Figure 10). This can be attributed to the covalent effect of Ce-O bonds. Because the number of cation coordination (CN = 7, 9) in X $_1$ -Y $_2$ SiO $_5$ is greater than that (CN = 6, 7) in X $_2$ -Y $_2$ SiO $_5$ [9]. In addition, the crystal lattice of X $_2$ -Y $_2$ SiO $_5$ is



a) X_1 -Y $_2$ SiO $_5$:Ce $^{3+}$ 1050°C

b) X_2 -Y $_2$ SiO $_5$:Ce $^{3+}$ 1250°C

Figure 4: Surface SEM morphology of X $_1$ -Y $_2$ SiO $_5$:Ce $^{3+}$ and X $_2$ -Y $_2$ SiO $_5$:Ce $^{3+}$ powders.

more rigid than that of X_1 - Y_2SiO_5 , which also makes a difference in luminescence intensity between them [10].

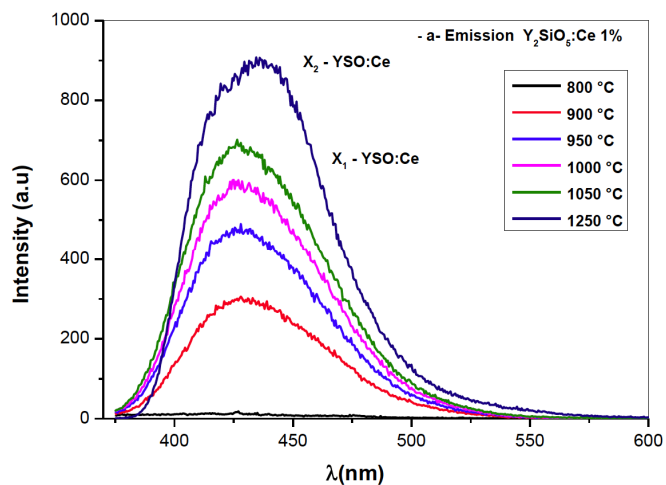


Figure 5: Emission spectra of $Y_2SiO_5:Ce^{3+}$ powders annealing at different temperatures.

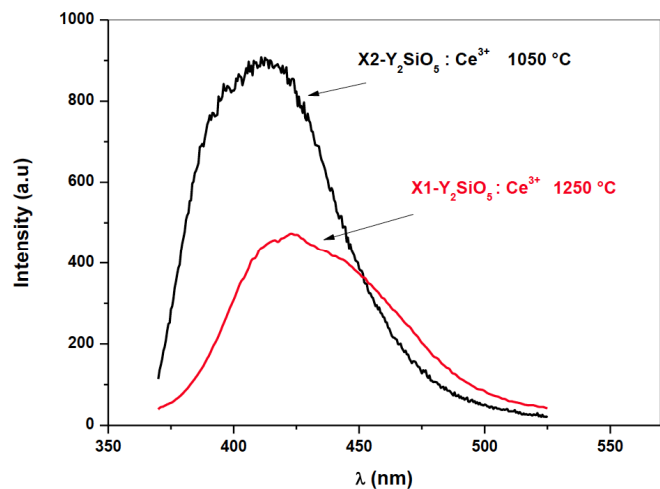


Figure 6: Emission spectra of X_1 - $Y_2SiO_5:Ce^{3+}$ (1050 °C) and X_2 - $Y_2SiO_5:Ce^{3+}$ (1250 °C).

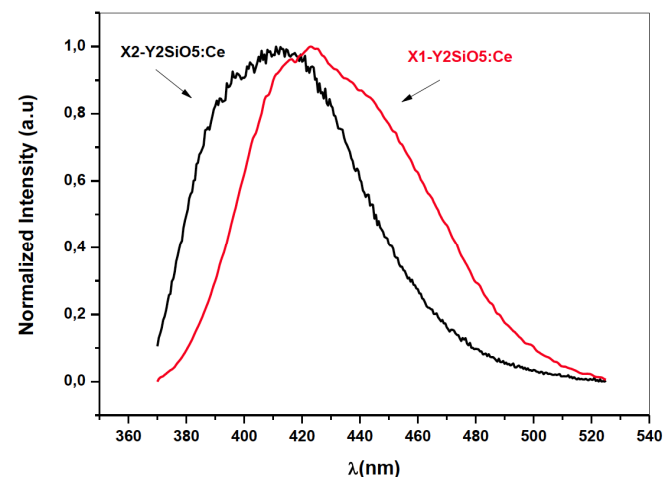


Figure 7: Normalized Emission spectra of X_1 - $Y_2SiO_5:Ce^{3+}$ (1050 °C) and X_2 - $Y_2SiO_5:Ce^{3+}$ (1250 °C).

Figure 8 shows the measured excitation spectra followed by an emission wave 420 nm, which corresponds to the interconfiguration transition $5d \rightarrow 4f$ ($^2F_{5/2}$, $^2F_{7/2}$) of Ce^{3+} . The excitation spectra are constituted by two absorption bands; A wide band located at about 360 nm and a low band centered at 276 nm.

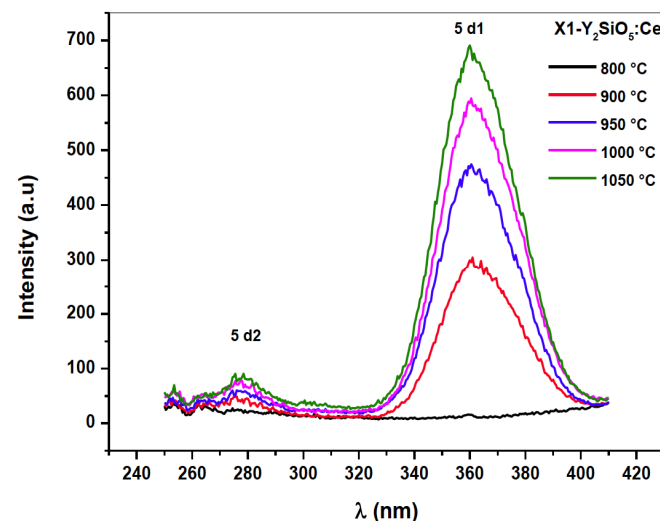


Figure 8: Excitation spectra of X_1 - $Y_2SiO_5:Ce^{3+}$ powders annealing at different temperatures.

The two excitation spectra of the Ce^{3+} doped Y_2SiO_5 samples annealed at 1050 °C and 1250 °C in the 250-450 nm range measured by a 420 nm emission wavelength at room temperature are shown in Figure 9. Two bands of absorption are observed: a very intense and very wide band whose maximum intensity is at 360 nm and another strip of much lower intensity at 300 nm. These bands are attributed to the electric dipole transitions allowed by the spin from the fundamental

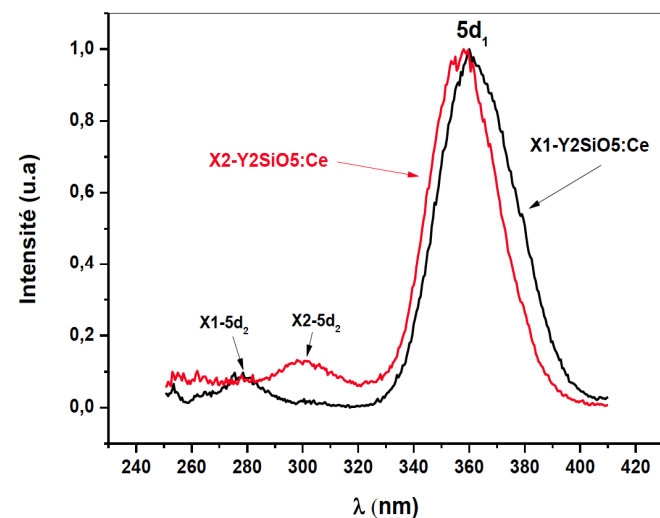


Figure 9: Normalized excitation spectra of the two phases X_1 - $Y_2SiO_5:Ce^{3+}$ (1050 °C) and X_2 - $Y_2SiO_5:Ce^{3+}$ (1250 °C).

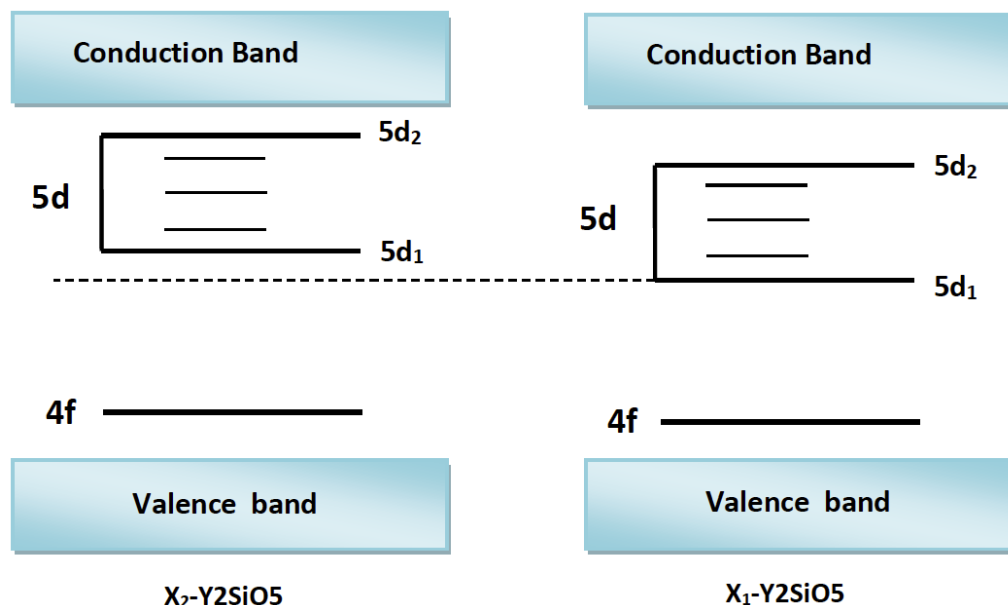


Figure 10: Energy levels of cerium in the two X_1 and X_2 phases of the Y_2SiO_5 structure.

level $4f$ ($^2F_{5/2}$) to the excited states $5d$ [11]. Under the effect of the crystalline field, we have a degeneracy lift of the $5d$ configuration in 5 sub-levels: the two lowest sub-levels, which we will call levels $5d_1$ and $5d_2$ (also noted levels $^2D_{3/2}$ and $^2D_{5/2}$).

4. CONCLUSION

In this work we have successfully synthesized the nanophosphors of the two monoclinic structures of Y_2SiO_5 X_1 and X_2 of groups of space $P2_1/c$ and $C2/c$ by simple sol gel method assisted by organic complex Ethylene glycol. We have experimentally studied the difference between these two structures and photoluminescence properties. It has been found that, despite the increase in temperature, the size of the crystallites still remains the same value around 41 nm in the range 900 - 1050 °C and which is explained by the absence of a coalescence phenomenon. The emission of cerium (Ce^{3+}) in X_1 - Y_2SiO_5 was found to increase with increasing annealing temperature. This phenomenon has been assigned to the improvement of crystallinity quality, which leads to a substitution of the Ce^{3+} ions in the Y^{3+} sites in the crystal lattice. The sample of X_2 - $Y_2SiO_5:Ce^{3+}$ (annealed at 1250 °C) exhibits larger crystallite sizes (~ 88 nm) compared with samples of X_1 - $Y_2SiO_5:Ce^{3+}$ (~ 41 nm). This is because of the annealing temperature which gave significant growth compared to X_1 - $Y_2SiO_5:Ce^{3+}$. The crystal lattice of X_2 - Y_2SiO_5 is more rigid than that of X_1 - Y_2SiO_5 and the emission intensity of the X_1 - $Y_2SiO_5:Ce^{3+}$ phase is much lower than that of the X_2 - $Y_2SiO_5:Ce^{3+}$ phase.

ACKNOWLEDGEMENT

This work was supported by Centre de Recherche Scientifique et Technique en Analyses Physico-Chimiques, BP 384, Zone Industrielle, Bou-Ismaïl CP 42004, Tipaza, Algeria.

REFERENCES

- [1] Aitasalo T, Holsa J, Lastusaari M, Niittykoski J, Pelle F. Delayed luminescence of Ce^{3+} doped X_1 form of Y_2SiO_5 . *Opt Mater* 2005; 27: 1511-1515. <https://doi.org/10.1016/j.optmat.2005.01.009>
- [2] Lu Q, Liu Q, Wei Q, Liu G, Zhuang J. Preparation and characterization of $Lu_2SiO_5:Ce^{3+}$ luminescent ceramic fibers via electrospinning. *Ceram Int* 2013; 39: 8159-8164. <https://doi.org/10.1016/j.ceramint.2013.03.090>
- [3] Jiao H, Gao X, Wang F, Wu A, Han T. Self-assembled Y_2SiO_5 superstructures: A high temperature method with mixed flux. *J Alloys Compd* 2010; 493: 427-430. <https://doi.org/10.1016/j.jallcom.2009.12.117>
- [4] Hamroun MSE, Guerbous L, Bensafi A. Luminescent spectroscopy and structural properties of Ce^{3+} -doped low-temperature X_1 - Y_2SiO_5 material prepared by polymer-assisted sol-gel method. *Appl Phys A* 2016; 122: 321. <https://doi.org/10.1007/s00339-016-9790-7>
- [5] Antic Z, Krsmanovic R, Marinovic-Cincovic M, Mitric M, Dramic-anin MD. Rare-earth doped $(Lu_{0.85}Y_{0.15})_2SiO_5$ nanocrystalline powders obtained by polymer assisted sol-gel synthesis. *Radiation Measurements* 2010; 45: 475-477. <https://doi.org/10.1016/j.radmeas.2009.10.016>
- [6] Guerbous L, Derbal M, Chaminade JP. Photoluminescence and energy transfer of Tm^{3+} doped $LiIn(WO_4)_2$ blue phosphors. *J Lumin* 2010; 130: 2469-2475. <https://doi.org/10.1016/j.jlumin.2010.08.014>
- [7] Cannas C, Mainas M, Musinu A, Piccaluga G, Speghini A, Bettinelli M. Nanocrystalline luminescent Eu^{3+} -doped Y_2SiO_5 prepared by sol-gel technique. *Opt Mater* 2005; 27: 1506-1510. <https://doi.org/10.1016/j.optmat.2005.01.008>

- [8] Williamson GK, Hall WH. X-ray line broadening from filed aluminium and wolfram. *Acta Metall* 1953; 1: 22. [https://doi.org/10.1016/0001-6160\(53\)90006-6](https://doi.org/10.1016/0001-6160(53)90006-6)
- [9] Lin J, Su Q, Zbang H, Wang S. Crystal structure dependence of the luminescence of rare earth ions (Ce³⁺, Tb³⁺, Sm³⁺) in Y₂SiO₅. *Materials Research Bulletin* 1996; 31(2): 189-196. [https://doi.org/10.1016/0025-5408\(95\)00178-6](https://doi.org/10.1016/0025-5408(95)00178-6)
- [10] Qin X, Ju Y, Bernhard S, Yao N. Europium-doped yttrium silicate nanophosphors prepared by flame synthesis. *Materials Research Bulletin* 2007; 42: 1440-1449. <https://doi.org/10.1016/j.materresbull.2006.11.021>
- [11] Hamroun MSE, Bachari K, Guerbous L, Berrayah A, Mechernene L. Structural and optical properties of LSO scintillator-polymer composite films. *Optik - International Journal for Light and Electron Optics* 2019; 187: 111-116. <https://doi.org/10.1016/j.ijleo.2019.05.022>

Received on 12-11-2022

Accepted on 05-12-2022

Published on 31-12-2022

<https://doi.org/10.6000/1929-5995.2022.11.08>

© 2022 Hamroun *et al.*; Licensee Lifescience Global.

This is an open access article licensed under the terms of the Creative Commons Attribution License (<http://creativecommons.org/licenses/by/4.0/>) which permits unrestricted use, distribution and reproduction in any medium, provided the work is properly cited.